



OPEN NAT10 promotes hepatocellular carcinoma progression by modulating the ac4C-DDIAS-PI3K-Akt axis

Yue Tao^{2,5,6}, Leisheng Wang^{2,6}, Enhong Chen^{1,6}, Shuo Zhang¹, Dongjie Yang³, Wuqiang Chen¹, Youzhao He¹, Yuanlong Gu¹✉, Yong Mao^{2,4}✉ & Hao Hu^{1,2}✉

Primary liver cancer (PLC) is a prevalent tumor globally, ranking third in cancer-related mortality. The role of N4-acetylcysteine (ac4C) and N-acetyltransferase 10 (NAT10) in hepatocellular carcinoma (HCC) progression, migration, and invasion requires further elucidation. High NAT10 expression correlated with poor prognosis in HCC patients. Knockdown of NAT10 hindered HCC cell proliferation. AcRIP-seq screening revealed DDIAS as a significant downstream target of NAT10. Decreased NAT10 levels reduced DDIAS mRNA stability, leading to decreased proliferation, migration, and invasion of HCC cells upon DDIAS knockdown. Ectopic expression of DDIAS counteracted the effects of NAT10 knockdown by modulating the PI3K/AKT pathway. NAT10 was found to be elevated in HCC tissues compared to normal tissues, promoting HCC progression and correlating with shorter overall survival in patients. Mechanistically, NAT10 regulated HCC progression through the ac4C-DDIAS-PI3K-AKT axis.

Keywords Hepatocellular carcinoma, NAT10, Acetylation, ac4C, DDIAS, PI3K-AKT

Abbreviations

HCC	Hepatocellular carcinoma
T	Tumor
N	Normal
NC	Negative control
NAT10	N-acetyltransferase 10
5'-UTR	5' untranslated regions
DDIAS	DNA damage-induced apoptosis suppressor
3'-UTR	3' untranslated regions
acRIP	ac4C-RNA immunoprecipitation
CDS	The coding region
RIP	RNA immunoprecipitation

Primary Liver Cancer (PLC) ranks as the third deadliest malignant tumor and the sixth most common cancer globally, emphasizing its critical nature that demands immediate attention. PLC encompasses Hepatocellular Carcinoma (HCC) and Intrahepatic Cholangiocarcinoma (IHCC) as its primary pathological types, with HCC constituting a significant majority, ranging from 75 to 85%, while IHCC represents 10–15% of cases. In 2020, there were a staggering 905,677 newly reported PLC cases worldwide, resulting in the tragic loss of 830,180 lives. These statistics underscore the immense public health challenge posed by PLC and the pressing need to enhance prevention, diagnosis, and treatment strategies¹. The regions with the highest incidence of PLC are Asia and Africa², with China alone accounting for approximately half of all global PLC cases³. PLC is currently

¹Department of Hepatobiliary and Pancreatic Surgery, Affiliated Hospital of Jiangnan University, 1000 Hefeng Rd, Binhu District, Wuxi 214122, Jiangsu Province, China. ²Wuxi Medical College, Jiangnan University, Wuxi 214122, Jiangsu Province, China. ³Department of pathology, Affiliated Hospital of Jiangnan University, 1000 Hefeng Rd, Binhu District, Wuxi 214122, Jiangsu Province, China. ⁴Department of cancer diagnosis and treatment center, Affiliated Hospital of Jiangnan University, 1000 Hefeng Rd, Binhu District, Wuxi 214122, Jiangsu Province, China. ⁵Wuxi Ninth People's Hospital Affiliated to Soochow University, No.999 Liangxi Road, Binhu District, Wuxi, China. ⁶These authors contributed equally: Yue Tao, Leisheng Wang and Enhong Chen. ✉email: alan89515@163.com; 9812015252@jiangnan.edu.cn; hao.hu@ntu.edu.cn

the second leading cause of mortality and the fourth most common malignant tumor in China, raising serious health concerns. Liver cancer still poses a serious threat to people’s lives and well-being, even with recent improvements in comprehensive therapeutic therapies^{4,5}. However, the survival rate of patients has not been significantly improved^{6,7}, so it is important to explore the key molecular events driving the development and progression of this disease. This study will help in hepatocellular cancer early diagnosis and therapy.

The most successful therapeutic management strategies in current era of healthcare are identified by precision and the application of biomarker guidance. Remarkably, earlier research has shown that hepatocellular carcinoma is a genetically predisposed and epigenetic disorder marked by genetic susceptibility and the interaction of genetic and epigenetic variables at different phases of tumorigenesis and development^{8,9}. To date, more than 170 chemical modifications on RNAs have been reported, including m1A, m5 C, m6 A, and ac4C¹⁰. In the past few years, research in the field of RNA modification has mainly focused on the more abundant m6A modification. In 2018, Arango et al. reported for the first time that mRNAs possess a modification called N4-acetylcysteine (ac4C) and suggested that NAT10 is the “writer” protein responsible for mRNA acetylation¹¹.

The physiological functions and regulatory mechanisms of ac4C alteration are currently receiving increased attention in cancer research, particularly in the fields of colorectal¹² and gastric malignancies^{13–15}. Our team is committed to conducting research that identifies and describes new therapeutic targets that are closely linked to the advancement of disease and negative outcomes in HCC. There is still a need for more research because it is unknown exactly how epigenetic modifications affect the course of HCC. The purpose of this study was to look into how NAT10 may be involved in the genesis of HCC. Consequently, our study provided insight into the role of NAT10 and suggested a possible substitute strategy for the management of HCC.

Materials and methods

Clinical samples

77 HCC patients had surgical excision at the Jiangnan University Affiliated Hospital between 2021 and 2023. From these patients, fresh tumor tissues and matching HCC tissue specimens were taken. The tissue samples were kept in tissue stabilizers called RNA Keepers (Vazyme, China). The proteins extracted from frozen tissues were employed for Immunohistochemical (IHC) staining or western blotting (WB) to evaluate NAT10 expression in HCC. The Pathological diagnosis, clinical, and follow-up data were available for all the 77 cases (illustrated in Table 1). Each patient in this study provided written informed consent in alignment with the guidelines set forth in the Declaration of Helsinki. The study protocol was approved by the ethical review committee of the Affiliated Hospital of Jiangnan University (LS2023032).

Cell culture

The human HCC cell lines (HCCLM3, PLC/PRF/5, and Sk-Hep-1) and Human Hepatic Stellate Cells (LX-2) were purchased from the Zhongqiao Xinzhou Biotechnology Co., Ltd. (Shanghai, China). The human HCC cell line Huh7 was obtained from the Procell Life Science&Technology Co., Ltd. (Wuhan, China). All the media were supplemented with 10% fetal bovine serum (FBS, Gibco), 100 IU/ml penicillin, and 100 µg/ml streptomycin (NCM, Suzhou, China). All cells were cultured at 37 °C in a humidified atmosphere containing 5% CO₂. Depending on the conditions of the cell growth, the medium was changed once every two to three days, and the healthy cells were chosen for further studies.

RNA extraction and quantitative polymerase chain reaction (qPCR)

TRIzol (R401, Vazyme) was used to separate total RNA from cells in accordance with the manufacturer’s instructions. The acquired RNA was then used to create complementary DNA using Vazyme’s HiScript II Q Select RT SuperMix (#R23301). SYBR qPCR Master Mix (Q511-02, Vazyme) was used in the ABI Prism 7500 system to measure mRNA expression. After normalization to GAPDH, the 2^{−ΔΔCt} method was used to determine

Feature		Total	NAT10 expression		p value
			Low	High	
Sex	Male	64	7	57	0.594
	Female	13	1	12	
Age (year)	≤60	32	2	30	0.271
	>65	45	6	39	
TNM stage (AJCC)b	≤2	68	7	61	0.649
	>2	9	1	8	
Nerve invasion (n)	Absent	75	8	67	0.802
	Present	2	0	2	
Vascular invasion (n)	Absent	21	7	14	<0.001
	Absent	56	1	55	
Immunoreactive Score	1–4	74	8	66	<0.001
	5–12	3	0	3	

Table 1. Characteristics of 77 HCC patients according to their expression of NAT10.

the relative expression levels of the target gene in each group. The sequences of various primers used in the experiment have been listed in Supplementary Table S1.

Western blotting

HCC cells were collected and lysed in a pre-cooled whole protein lysate ice bath for 15–30 min. The total protein was extracted using RIPA cell lysate (ProteinBio, China), and then the total protein was resolved by sodium dodecyl sulfate-polyacrylamide gel electrophoresis (SDS-PAGE) gel. The treated sample was initially separated at 80 V for 30 min, then separated at 120 V for 60 min, and finally wet transferred to a polyvinylidene fluoride (PVDF) membrane. They were then treated with a blocking buffer (Beyotime, China) for 1–2 h and incubated overnight with primary antibody at 4 °C. On the 2nd d, after the secondary antibody was incubated for 1 h at room temperature, the data were collected with an ECL developer (Millipore, USA). The various antibodies used in this study have been listed in Supplementary Table 2.

Immunohistochemical (IHC) staining

The IHC assay was carried out in accordance with the specified protocol. In a nutshell, liver cancer tissues were embedded, clipped, and preserved in 4% paraformaldehyde. They were then fixed in paraffin, dehydrated by soaking in gradient ethanol, transparentizable in xylene, and sectioned into 4 µm tissue slices. For high-temperature antigen repair, 2% EDTA solution was added to the slices after they had been dewaxed with water. The endogenous peroxidase was eliminated using 3% H₂O₂, and then NAT10 and DDIAS antibodies (1:500, T510105/M051478, Abmart, China) were added. The mixture was then incubated at 4 °C for an overnight period before being cleaned with phosphate buffer saline (PBS). Wet box was placed in the refrigerator at 4 °C overnight, and the secondary antibody was incubated for 30 min. The samples were then stained and photographed. The IHC staining results were quantified by multiplying the proportion of immunoreactive cells by the intensity of staining. Staining intensity is generally divided into 3 levels, indicated by 1, 2 and 3, corresponding to no staining, light staining and heavy staining. The value of H-score ranges from 0 to 300, with higher scores indicating more intense staining results.

Stable cell line construction and cell transfection

Small interfering RNA (siRNA) specific to DDIAS, along with the corresponding negative control, was chemically synthesized by Sangon Biotech (Shanghai, China). To facilitate the transfection of the recombinant plasmids into hepatocellular carcinoma (HCC) cells, Lipofectamine 2000, a product of Thermo Fisher Scientific, was employed following the detailed protocol provided by the manufacturer. GeneChem (Shanghai, China) produced lentiviral packaging shNAT10 or shNC. HCC cell lines were treated with lentiviral particles, and they were then incubated for 48 h. With puromycin selection, the stable cell clones were produced¹⁶. DDIAS overexpression plasmids were purchased from Hengyu Biotech (Shanghai, China).

Transwell assay

The upper chamber (Corning, USA) was utilized for culturing HCC cells in suspension with serum-free medium at a concentration of 5 × 10⁴ cells per well. In contrast, the lower chamber contained medium supplemented with 10% FBS. Subsequently, the chambers were placed in an incubator for 24 to 72 h, after which the upper layer of uncrossed cells was wiped off, and the cells were fixed with fixative and stained. Finally, quantitative results of cell migration and invasion were obtained by microscopic observation and image analysis. For the invasion assay, the experimental setup closely resembled that of the migration assay, except for the application of Matrigel (BD Biosciences, USA) in the upper chamber. This additional step allowed for the assessment of invasive properties of the HCC cells. The same procedures for incubation, removal of cells from the upper chamber, fixation, staining, and microscopic analysis were carried out to evaluate the invasive potential of the HCC cells under study.

Cell proliferation assay

In line with the guidelines provided by the manufacturer, the CCK-8 Cell Counting Kit (Vazyme, China) was utilized for assessing cell proliferation. A 96-well plate was utilized, with 100 µl of cell suspension added to each well. Following this, each well was incubated for the recommended duration before 10 µl of CCK-8 solution was added. The mixture was then further incubated for an additional two hours. The optical density (OD) value of each well was subsequently measured using a microplate reader at a wavelength of 450 nm. The experimental procedure involved following the manufacturer's instructions to ensure accurate and reliable results.

Immunofluorescence

The procedure for immunofluorescence was as previously mentioned¹⁷. In summary, after being cleansed with PBS, HCCLM3 and Sk-Hep-1 cells were fixed with 4% PFA for 15 min at room temperature. After one more PBS wash, the cells were incubated in the appropriate antibodies for an entire night at 4 °C. The cells were then treated in fluorescein-labeled secondary antibodies for 30 min at 37 °C following another PBS wash. The cells were incubated with DAPI (Beyotime, China) after being cleaned three times more using PBS. A microscope was then used to examine the slides. The antibodies used in this experiment have been listed in Supplementary Table S2.

RNA sequencing (RNA-seq) and acRIP sequencing (acRIP-seq)

GeneChem (Shanghai, China) provided RNA sequencing services for NAT10 knockdown HCCLM3 cells and ac4C-RIP-Seq analysis for NAT10 knockout HCCLM3 cells and NC cells to identify ac4C modifications in HCC genes. Data analysis and processing were exclusively performed by GeneChem.

RNA immunoprecipitation (RIP)

The Magna RIP RNA-binding protein immunoprecipitation kit (Millipore, USA) was used for the RIP experiment following the manufacturer's instructions. Cells were collected and lysed using RIP lysis buffer. Subsequently, magnetic beads were individually treated with NAT10 antibody and anti-rabbit IgG (Millipore, Germany) for one to two hours at room temperature before adding cell lysates (approximately 2×10^7 cells per sample). Following washing, the spheres were incubated for three h at 4 °C with the cell lysis. Following the spheres' collection and washing, phenol-chloroform extraction was used to separate the RNA compound. For the RNA-rich regions, a quantitative polymerase chain reaction was used. We improved the Magna meriptmm6A kit (17-10499, Millipore) methodology for the acRIP analysis of NAT10 knockdown by substituting the ac4C antibody (ab252215, Abcam) for the m6A antibody. The reagent instruction manual was followed in conducting the complete method. All the target sequences have been shown in Supplementary Table S1.

RNA decay assay

We further assessed the potential impact of NAT10 on the stability of DDIAS mRNA using the RNA degradation test. The HCCLM3-shNC, HCCLM3-shNAT10-2, Sk-Hep-1-shNC, and Sk-Hep-1-shNAT10-2 cells were grown in 6-well dishes. Actinomycin D (HY-17559, MCE) was then included in each dish at a final dose of 5 µg/ml. The cells were harvested after 0, 2, 4, 6, and 8 h, respectively. Total RNA was extracted and analyzed using RT-qPCR to measure the relative levels of DDIAS mRNA.

Statistical analysis

The statistical analysis of the data was conducted and the results were presented as mean \pm standard deviation using GraphPad Prism 9.0. The data were assessed using a two-tailed Student's t-test for comparison between two groups, and a one-way ANOVA for multiple comparisons. The survival rate of HCC patients was determined using a Kaplan-Meier curve. Significant differences were indicated as $P < 0.05$ (*), $P < 0.01$ (**), and $P < 0.001$ (***).

Results

NAT10 is highly expressed in HCC and negatively correlates with prognosis

Using the GEPIA database, we looked at NAT10 expression in HCC to look into the expression profile of NAT10 (<http://gepia.cancer-pku.cn/>), which showed that NAT10 mRNA expression in HCC tissues was significantly higher than that in adjacent normal tissues ($P < 0.05$) (Fig. 1A). Furthermore, patients with HCC who expressed more NAT10 had worse progression-free survival (PFS) and overall survival (OS) (Fig. 1B). The Cancer Genome Atlas (TCGA) database results have further reinforced the notion that NAT10 expression serves as a significant factor in determining the prognosis of individuals diagnosed with early-stage Hepatocellular Carcinoma (HCC). This research indicates that NAT10 expression levels can be utilized as a reliable indicator for forecasting the survival outcomes of such patients. With this validation from TCGA data, the importance of NAT10 as a prognostic marker in early-stage HCC becomes even more pronounced (Fig. 1C). We next analyzed the protein levels of NAT10 in 6 pairs of HCC tissues, and immunoblotting results revealed that NAT10 protein levels were upregulated in cancerous tissues compared to both adjacent cancerous tissues and normal tissues (Fig. 1D). NAT10 expression (Fig. 1E,F) was then further determined by immunohistochemical staining of tissue microarrays (TMAs) consisting of 77 pairs of HCC and non-tumor samples. Depending on their NAT10 levels, patients with HCC were split into two groups. It was found that by December 2023, there were nine deaths, five metastases, and two recurrences in 77 patients with HCC, yielding a median progression-free survival (PFS) of 350 d (301-654d). The Kaplan-Meier survival curve indicated a negative association between NAT10 expression and PFS ($P = 0.007$) (Fig. 1G). The clinical association studies revealed a significant correlation between NAT10 expression and histologic grading (Table 1). NAT10 dysregulation may have a role in the development of HCC, according to these results.

NAT10 affected HCC proliferation, migration, and invasion in vitro

We first looked at NAT10 expression in HCC cell lines in order to assess the functional relevance of NAT10 in HCC (Supplementary Material Fig.S1A,B). Sk-Hep-1 and HCCLM3 cells were selected to establish NAT10 silencing models. We performed NAT10 knockdown experiments in SK-Hep-1 and HCCLM3 cells. A specific shRNA targeting NAT10 was generated to knock down NAT10 expression. The qPCR and western blot analysis revealed that shRNA significantly reduced mRNA and protein expression of NAT10 in HCC cells transfected with shRNA, thereby indicating good knockdown efficiency (Fig. 2A,B). Based on the results of CCK-8 assays, the knockdown of NAT10 significantly decreased the proliferative capacity of HCC cells (Fig. 2C). We performed transwell assays and found that knockdown of NAT10 inhibited the ability of HCC cells to migrate and invade (Fig. 2D,E). Overall, in vitro conditions saw less HCC cell invasion, migration, and proliferation as a result of NAT10 downregulation.

ac4C-seq combined with RNA-seq revealed DDIAS as a target of NAT10

Acetylated RNA immunoprecipitation was employed to investigate how NAT10 promotes HCC malignancy, alongside RNA sequencing conducted on HCCLM3 cells with NAT10 knockdown and control (NC) cells. A heatmap showcasing genes that were expressed differently in HCCLM3 cells following treatment with either NC or following knockdown of NAT10 (Fig. 3A). The ac4C signaling was found to be enriched around the CDS and 3' UTR of the mRNAs (Fig. 3B). Moreover, peak distribution analysis of the transcripts revealed that one to three ac4C was present in the majority of mRNAs (Fig. 3C). The screening criteria for both sequencing results were set at $|\log_2\text{FC}| > 1$ and a P -value of 0.05. The differences in mRNA gene expression were illustrated using a Venn diagram, which revealed 461 genes in the RNA-seq results and 1,232 genes in the ac4CRIP-seq results.

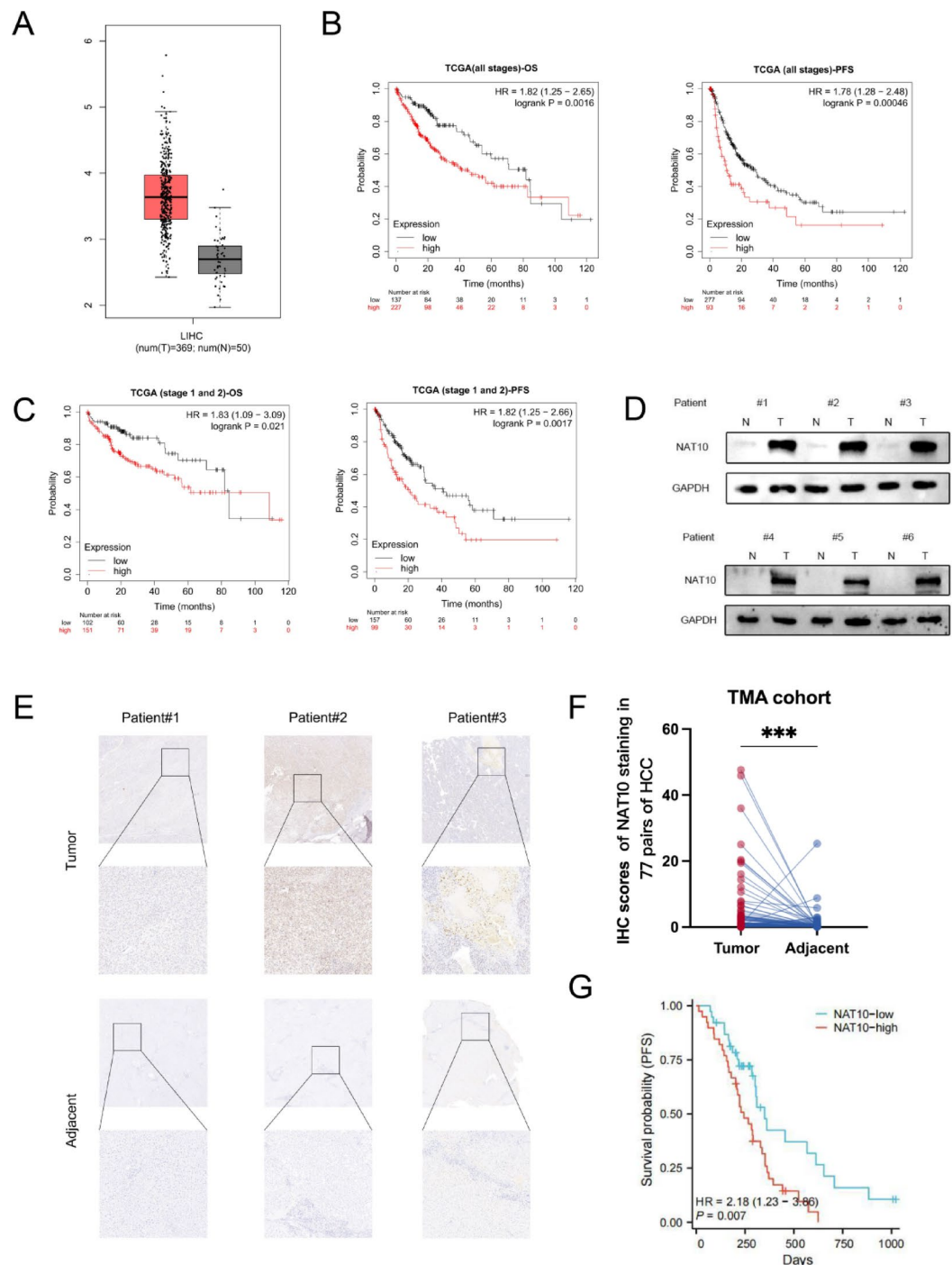


Fig. 1. NAT10 was highly expressed and prognostic values in HCC. **(A)** The web-based tool GEPIA was utilized to investigate NAT10 mRNA expression levels in HCC tissues. **(B)** The Kaplan-Meier plotter, an online resource, was used to determine the relationship between NAT10 mRNA expression and overall survival (left) and progression-free survival (right) in HCC patients. **(C)** Kaplan-Meier survival analysis was conducted based on NAT10 expression in early-stage HCC patients (from TCGA cohort, stages 1 and 2). **(D)** Western blot analysis was performed on six HCC sample pairs to assess NAT10 expression. **(E)** Representative images depicting NAT10 IHC staining in HCC samples were presented, with scale bars measuring 100 μ m. **(F)** IHC scores for matched HCC and normal tissues ($n=77$) were calculated based on NAT10 staining. **(G)** Kaplan-Meier analysis of HCC patient progression-free survival relative to NAT10 expression levels was carried out ($n=77$). The median of IHC scores served as the cutoff for group classification. Knockdown of NAT10 was observed to inhibit proliferation, migration, and invasion capacities in HCC cells during in vitro studies. **(A, B)** RT-qPCR and Western blot assays confirmed NAT10 expression levels in shNAT10 HCC cells. **(C)** The CCK8 assay assessed the impact of NAT10 knockdown on the proliferation of HCC cells. **(D, E)** Transwell assays evaluated the effect of NAT10 knockdown on the migratory **(D)** and invasive **(E)** abilities of HCC cells, with a scale bar of 200 μ m.

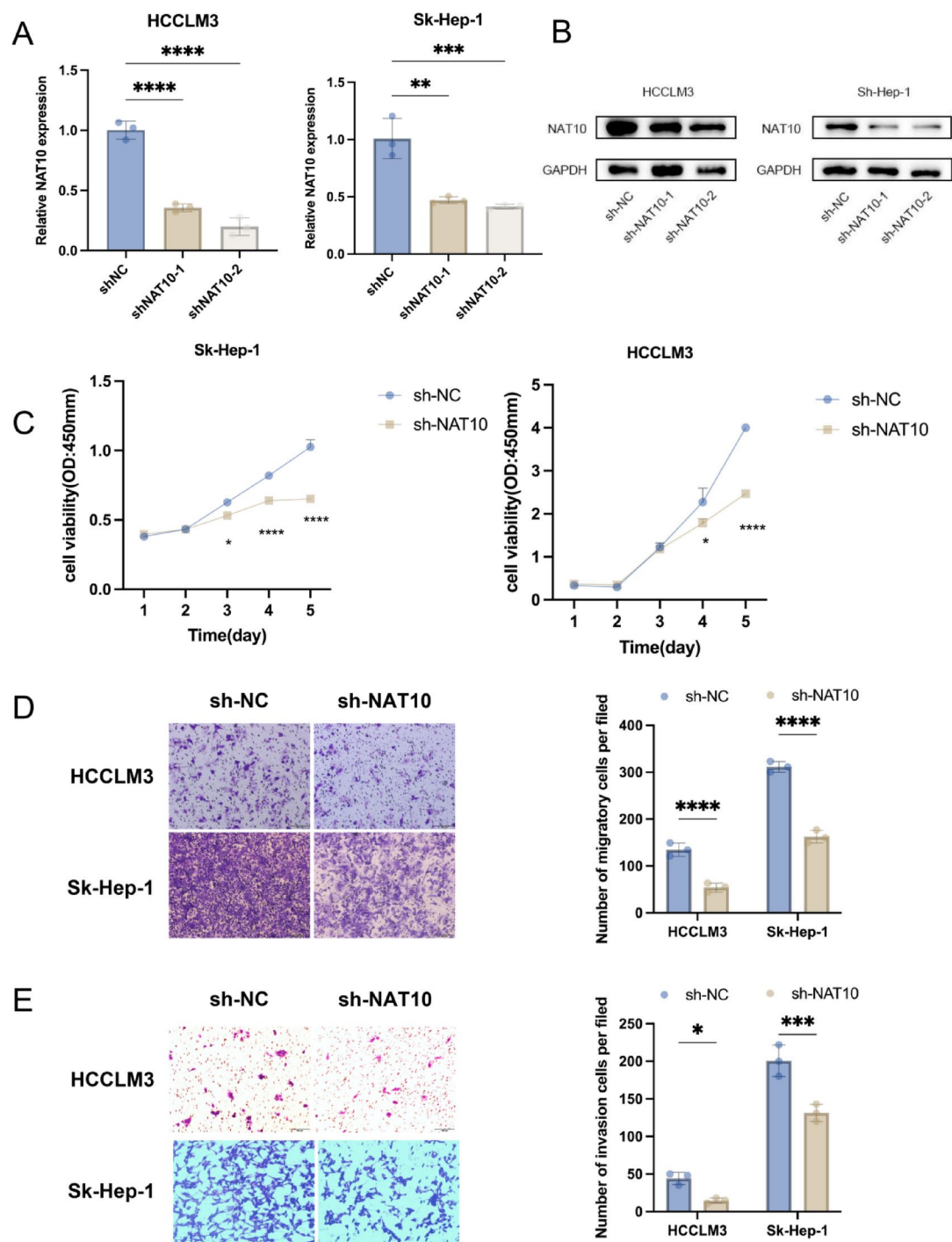


Fig. 2. Knockdown of NAT10 hindered the proliferation, migration, and invasion capabilities of HCC cells in vitro. (A, B) RT-qPCR and Western blotting assays were used to verify NAT10 expression in shNAT10 HCC cells. (C) The CCK8 assay was employed to explore the influence of NAT10 knockdown on the proliferative capacity of HCC cells. (D, E) Transwell assays were conducted to scrutinize the impact of NAT10 knockdown on HCC cell migratory (D) and invasive (E) capacities. Scale bar: 200 μ m.

(Fig. 3D). In particular, we were interested in studying the oncogenes' acetylation pattern and the controlled NAT10's expression. Consequently, only the mRNAs that showed reduced levels of acetylation and expression after NAT10 knockdown were selected for further examination. (Fig. 3E). The crossover results showed ten, including DDIA5. Furthermore, further analysis of the data showed that the ac4C peak found in DDIA5 was situated on chromosome 11 at the region of 82,932,313–82,932,494 (+) (Fig. 3F).

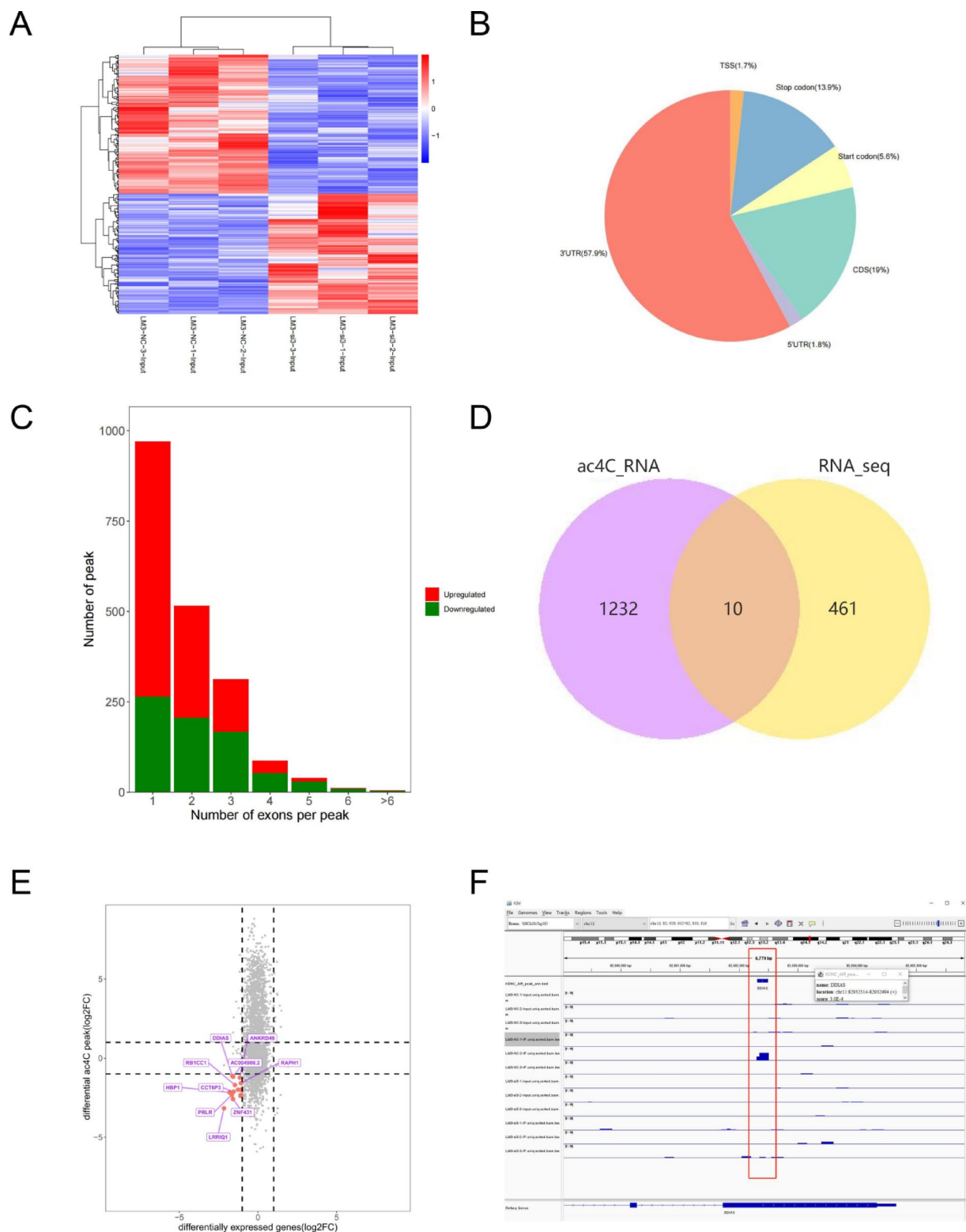


Fig. 3. ac4C-seq and RNA-seq analysis demonstrated NAT10 as a potential target of DDIAS. **(A)** RNA-sequencing was utilized to examine the differential gene expression in HCCLM3 cells transfected with either NC or NAT10 shRNA. **(B)** The ac4C peaks were predominantly found within the CDS and 3'UTR regions of HCC cells. **(C)** The proportion of mRNAs containing varying quantities of ac4C peaks was determined. **(D)** A Venn diagram was utilized to identify the mRNAs exhibiting alterations in both ac4C peak levels and gene expression. **(E)** The star plot displayed the distribution of genes showing differential ac4C peaks (hyper or hypo; Y-axis; fold change > 1.5 or 2 or < 0.5, $P < 0.05$) in the NAT10-downexpressing group compared to the control group. **(F)** The location of the ac4C peak on DDIAS was analyzed using IGV.

NAT10 regulated the expression of DDIAS in an N4-acetylcytidine-dependent manner

Based on the acRIP-seq analysis, a substantial decrease in the DDIAS ac4C peak in the CDS region was linked to decreased expression of NAT10. The role of NAT10 in enhancing DDIAS mRNA levels was confirmed using RIP assays with an anti-NAT10 antibody on Sk-Hep-1 and HCCLM3 cells, indicating that NAT10 regulation may occur at the RNA level upon interaction (Fig. 4A). Additionally, reduction of NAT10 might effectively diminish ac4C modification of DDIAS in the CDS region, according to acRIP-qPCR experiments using primers targeting putative ac4C sites (Fig. 4B). According to reports¹¹, the ac4C peak in the swing site enhances translation efficiency, and the NAT10 enzyme promotes mRNA stability. NAT10 confers the enzyme acetyltransferase to improve mRNA stability, and translation efficiency is stimulated by the ac4C peak located within the swing site. It was discovered that NAT10 deficiency caused DDIAS mRNA to degrade more quickly (Fig. 4C). Furthermore, NAT10 mRNA expression in HCC tissues was strongly correlated with DDIAS levels, according to data from the TCGA database (Fig. 4D). It's interesting to note that following NAT10 knockdown, DDIAS mRNA and protein expressions in cells dramatically dropped (Fig. 4E,F). The co-localization of NAT10 and DDIAS in the nuclei of HCCLM3 and Sk-Hep-1 was verified by the immunofluorescence test (Fig. 4G). The findings demonstrated that NAT10 regulated DDIAS expression in an ac4C-dependent manner.

DDIAS promoted HCC proliferation and invasion

Using the TCGA database, the mRNA expression level of DDIAS was validated, revealing a significant increase in DDIAS expression in hepatocellular carcinoma tissues when compared to corresponding normal tissues. (Fig. 5A). Additionally, progression-free survival (PFS) and overall survival (OS) were lower in HCC patients with high DDIAS expression (Fig. 5B). The findings from the Cancer Genome Atlas (TCGA) database provided additional validation for this conclusion. This result was supported by the discovery that, in contrast to Human Hepatic Stellate Cells, DDIAS mRNA (Fig. 5C) and protein (Fig. 5D) were expressed at higher levels in four different HCC cell lines. Furthermore, further immunohistochemical labeling was used to confirm the findings (Fig. 5E). To investigate the function of DDIAS in HCC further, DDIAS knockdown was performed in HCCLM3 and Sk-Hep-1 cells. DDIAS knockdown significantly decreased the proliferation, migration, and invasion of HCCLM3 and Sk-Hep-1 cells (Fig. 6A–D). According to these results, DDIAS controls how quickly HCC progresses.

NAT10 regulated HCC proliferation and invasion by the DDIAS-PI3K-Akt pathway

Research has shown that the PI3K-Akt pathway can be regulated by NAT10¹⁸. In our analysis of PI3K-Akt pathway protein expression using Western blotting, we found that the levels of PI3K, Akt, and their phosphorylated forms (Tyr467/199 and Ser473) were significantly reduced in both HCCLM3 and Sk-Hep-1 cells (Fig. 6E). However, NAT10 knockdown substantially decreased PI3K and AKT phosphorylation levels in HCCLM3 and SK-Hep-1 cells (Fig. 6F). In order to investigate whether DDIAS operates independently of NAT10, we carried out an experiment in which DDIAS was overexpressed in the absence of NAT10 (Fig. 7A–D). Furthermore, it was observed that DDIAS overexpression induced a rise in PI3K and AKT phosphorylation levels, which was a consequence of NAT10 knockdown. This suggests that DDIAS overexpression triggered the PI3K/AKT pathway (Fig. 7E).

Discussion

In this work, we discovered that NAT10 directly enhances the translation of the DDIAS protein, resulting in increased mRNA acetylation. This modification subsequently alters the PI3K-AKT pathway, ultimately promoting the proliferation of hepatocellular carcinoma cells (Fig. 8). The lack of understanding of the exact molecular mechanisms of hepatocellular carcinoma occurrence and progression has severely limited the exploration of new strategies for the effective treatment of hepatocellular carcinoma. HCC is the second most common cause of cancer-related deaths and its incidence is on the rise globally¹⁹. Although surgical and local topical treatments are widely used worldwide²⁰, it is estimated that 50–60% of HCC patients will eventually receive systemic therapy²¹. According to our research, NAT10 may present a viable therapeutic target for the management of liver cancer. In the present study, we discovered that NAT10 levels are significantly increased in HCC tissues, suggesting a potential association between ac4C modification and the development of HCC. In this study, we combined data from the GEPIA database with immunohistochemical staining of pathological sections obtained from our hospital and found that HCC patients with high NAT10 levels had shorter overall survival. Previous studies have shown similar findings^{18,22}. The study of epigenetic modification—more especially, RNA methylation modification, including m6A methylation, which was the primary focus of our earlier work—has gained attention in recent years due to the development of high-throughput sequencing technology.

Both prokaryotic and eukaryotic species have conserved the chemical alteration N4-acetylcysteine. Since NAT10 is a recently identified RNA alteration, more research has been done on its mechanism and function. NAT10 has been implicated in a variety of disorders, supporting its significance in disease mechanisms. For example, earlier research has highlighted the relationship between NAT10 and Hutchinson-Gilford progeria syndrome, a condition characterized by accelerated aging. Studies have demonstrated that reducing NAT10 expression can significantly restore the balance of non-classical nuclear transportin-1 (TNPO1) within the nucleus and cytoplasm. This adjustment in the nucleoplasmic ratio of TNPO1 leads to an improved nuclear mass ratio in individuals with progeria, thereby ameliorating some of the cellular abnormalities associated with this premature aging disorder^{22,23}. We have effectively created stable cell lines with modified NAT10 expression for our investigation. Next, we investigated the effects of NAT10 expression on HCC cell migration and invasion capacity as well as HCC metastasis. The results revealed that NAT10 promoted both invasion and migration of hepatocellular carcinoma cells, which was consistent with the previous studies^{24,25}. In addition, we analyzed the potential relationship between NAT10 expression and clinical prognosis in HCC patients registered at our

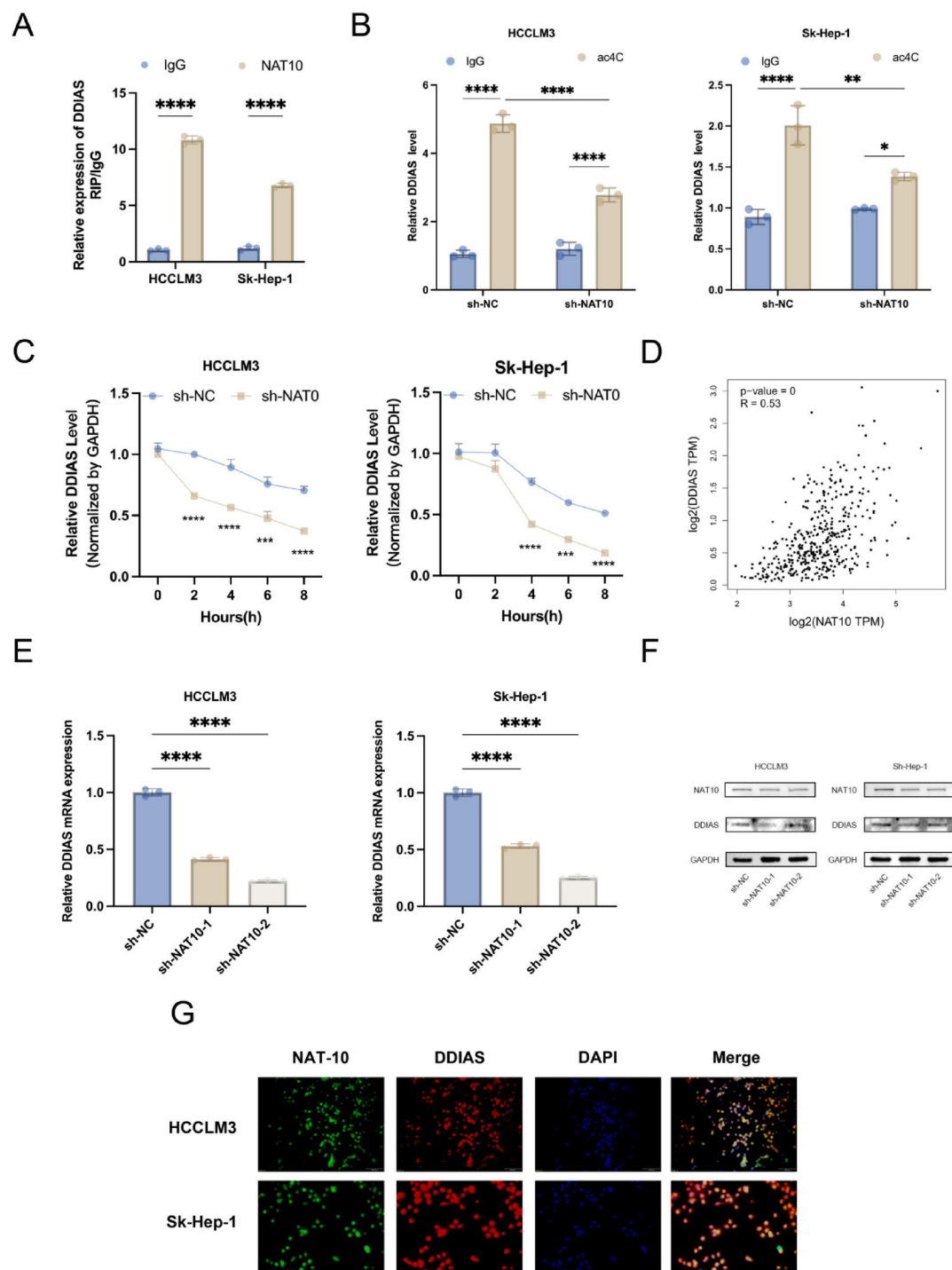


Fig. 4. NAT10 controlled DDIAS expression in an acetylation-dependent manner. **(A)** Binding capacity between DDIAS mRNA and NAT10 in HCC cells was determined using RIP assay. **(B)** acRIP-qPCR was used to analyze the impact of NAT10 knockdown on acetylation levels of DDIAS in HCC cells. **(C)** qPCR was performed to examine the effect of NAT10 knockdown on DDIAS half-life in HCC cells. **(D)** The relationship between DDIAS and NAT10 expression in The Cancer Genome Atlas database for HCC was investigated. **(E)** qPCR was utilized to analyze the changes in DDIAS mRNA expression upon NAT10 knockdown. **(F)** DDIAS protein levels were measured post-NAT10 knockdown. Data was presented as means \pm SD. **(G)** Immunofluorescence assay showed co-localization of NAT10 (green) and DDIAS (red) with DAPI (blue) staining marking the nucleus (scalebar = 100 μ m).

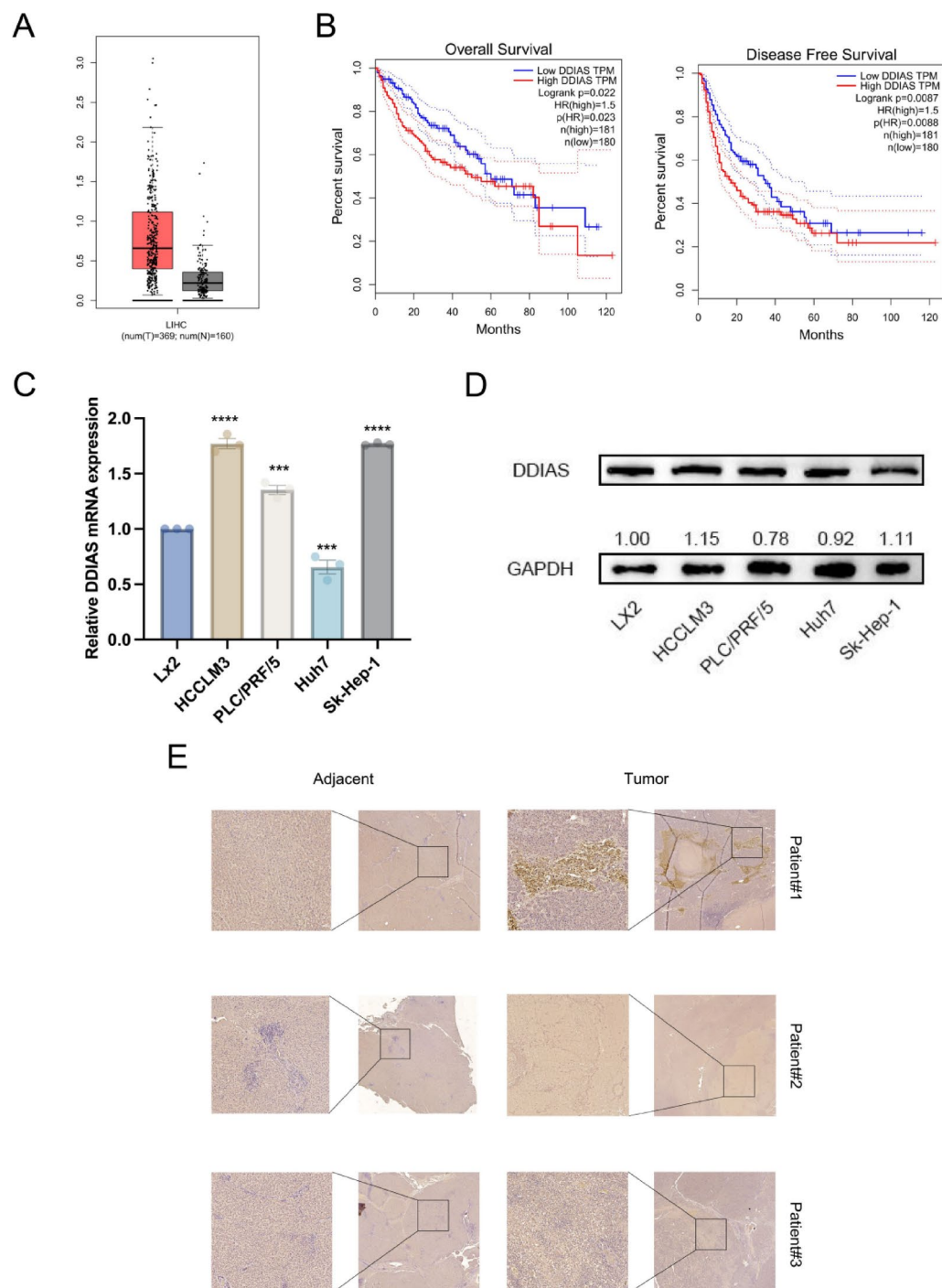


Fig. 5. DDIAS facilitated both the proliferation and invasion of HCC. **(A)** DDIAS mRNA levels were evaluated in HCC tissues using the GEPIA online tool. **(B)** The potential correlation between DDIAS mRNA expression and overall survival (left) as well as progression-free survival (right) in HCC was examined via the Kaplan-Meier plotter online tool. **(C, D)** qPCR **(C)** and western blot assays **(D)** were utilized to measure DDIAS expression in HCC cells and Lx2 cells. **(E)** Representative images displaying DDIAS IHC staining in HCC samples were presented (scale bars: 100 μ m).

institution, which aligns with the results of external databases. Our findings demonstrated for the first time that NAT10 can, in an ac4C-dependent manner, promote cancer in HCC. Ac4C modification plays a crucial role in several regulatory processes that are vital for proper cellular functioning. Firstly, it is involved in enhancing RNA stability, ensuring that RNA molecules remain intact and functional for the necessary duration within the cell. Additionally, ac4C modification is integral to RNA decay processes, where it helps in the systematic breakdown and recycling of RNA molecules, thereby maintaining cellular homeostasis. Furthermore, this

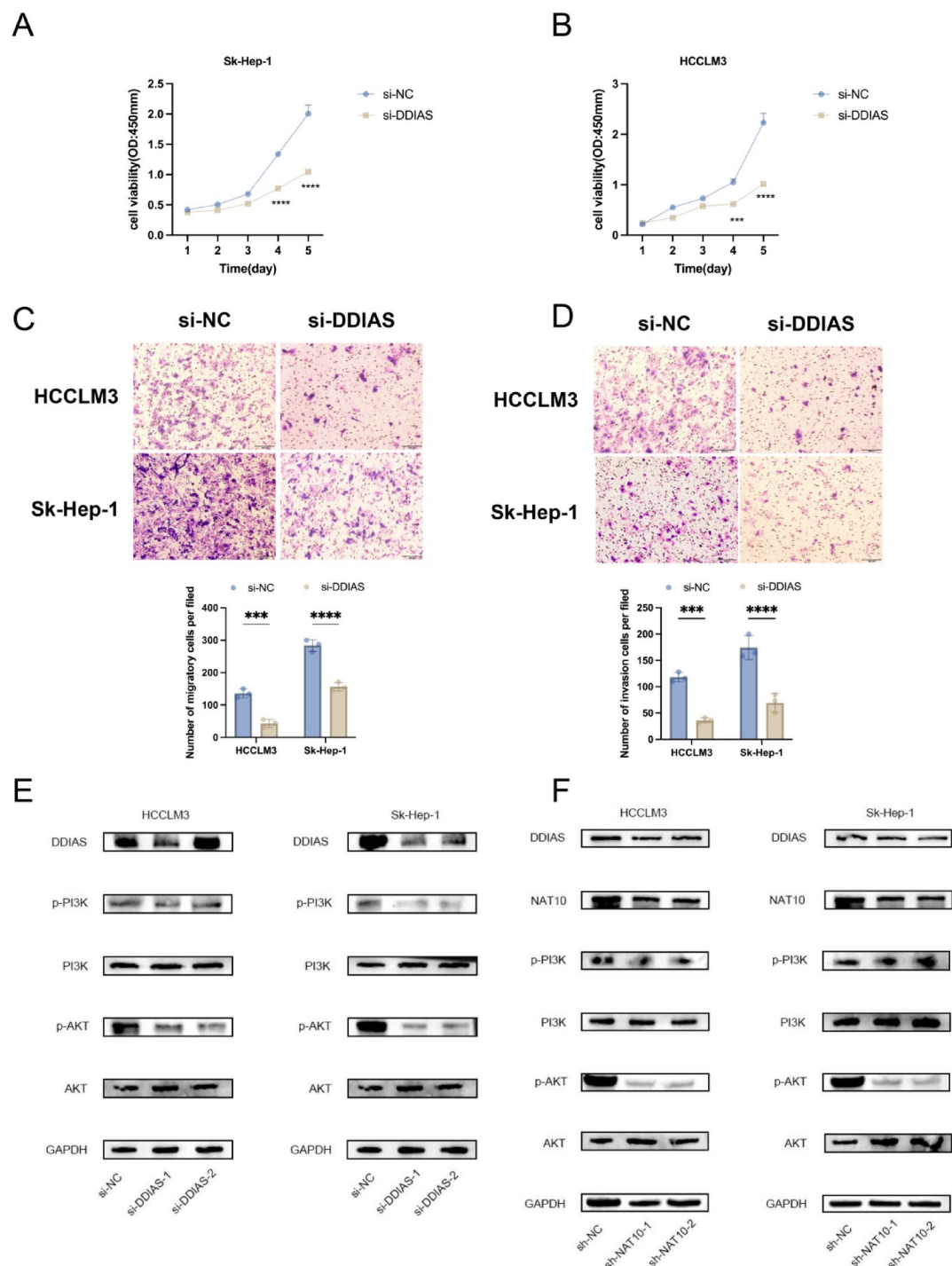


Fig. 6. By influencing the DDIAS-PI3K-AKT pathway, NAT10 controlled the invasion and proliferation of HCC. (A, B) Using the CCK8 assay, the impact of DDIAS knockdown on the ability of HCC cells to proliferate was investigated (C, D) Using a transwell experiment, the effect of DDIAS knockdown on the migratory (C) and invasive (D) potential of HCC cells was investigated. Scale bar: 200 μ m. (E, F) Activation of PI3K/Akt signaling pathway as detected after (E) DDIAS knockdown or (F) NAT10 knockdown in HCCLM3 and Sk-Hep-1 cells.

modification significantly contributes to nuclear retention by aiding in the retention of specific RNA molecules within the nucleus, preventing their premature export to the cytoplasm. Lastly, ac4C modification is essential in the translation process, facilitating the efficient and accurate synthesis of proteins from RNA templates. Through these various roles, ac4C modification underscores its importance in the complex network of gene expression regulation^{26,27}. These results Our knowledge of the functional and downstream regulatory processes of ac4C

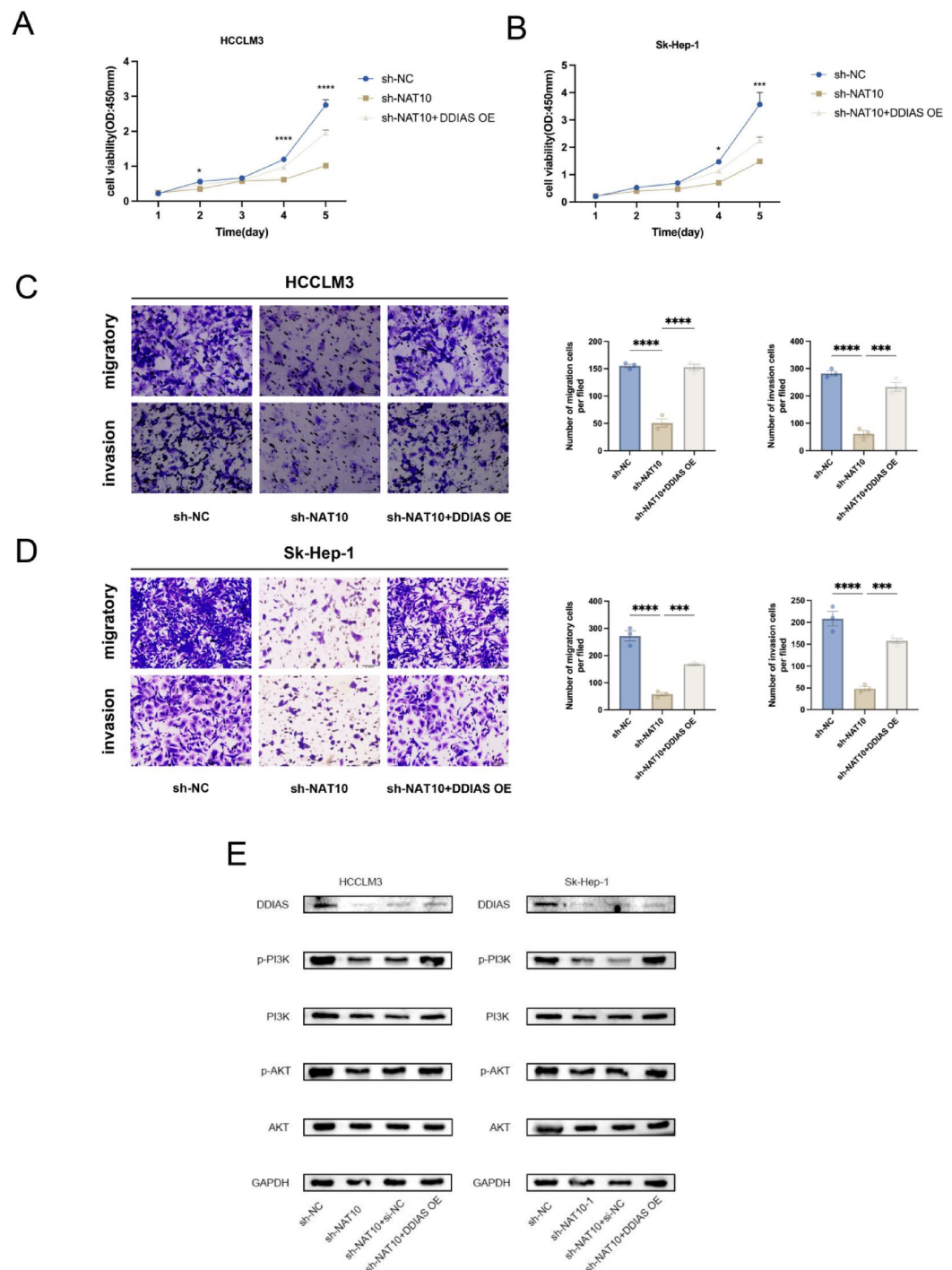


Fig. 7. The schematic below depicts the role NAT10 plays in modulating PI3K/Akt signaling in HCC progression. (A, B) CCK8 assay was used to examine the reversal effect of DDIAS overexpression on proliferative capacity of shNAT10 HCC cells. (C, D) Transwell assays were used to determine the reversal effects of DDIAS overexpression on the migratory (C) and invasive (D) capacities of shNAT10 cells. Scale bar: 100 μ m (E) Western blot analysis was conducted to assess the impact of DDIAS overexpression on the protein levels of key Akt pathway components in hepatocellular carcinoma cells.

acetylation is expanded by these findings. These findings verified the role of NAT10 in cancers such as HCC. Hence, targeting NAT10 presents a novel therapeutic approach to cancer treatment.

We discovered that DDIAS may be NAT10's downstream target by using an ac4C epitranscriptomic sequencing investigation. Interestingly, NAT10 knockdown significantly diminished the ac4C levels of DDIAS and suppressed the increase in DDIAS mRNA, ultimately leading to a decrease in DDIAS expression. Our current investigation found that DDIAS was significantly reduced by NAT10 knockdown. The direct interaction

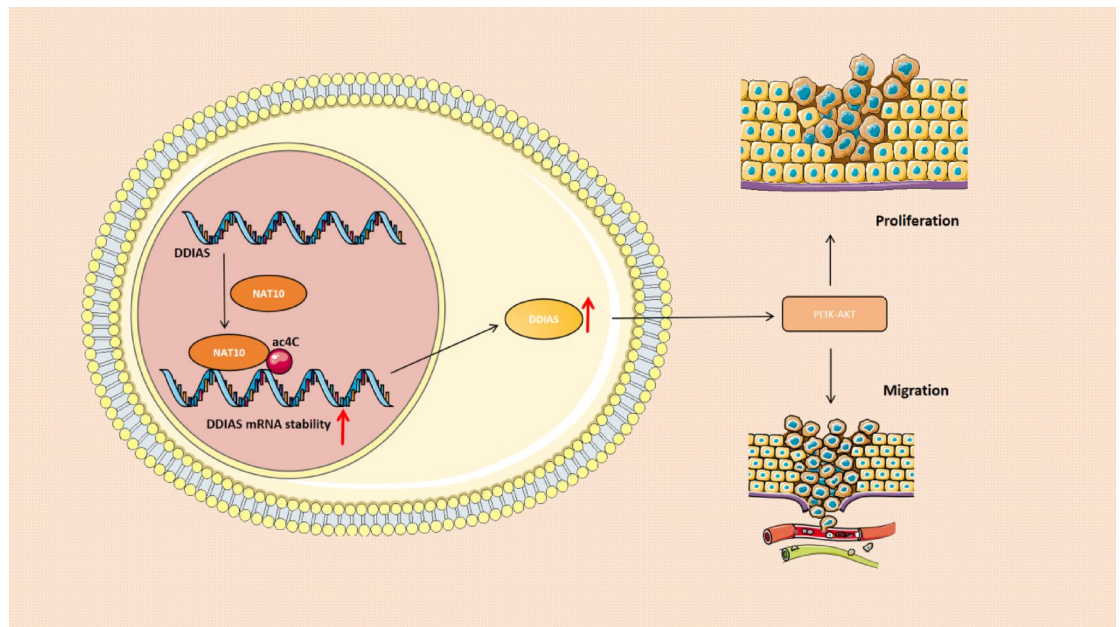


Fig. 8. A diagram demonstrates that NAT10 has the potential to be a valuable focus for enhancing HCC treatment by acetylating and stabilizing DDIAS mRNA to boost its levels and regulate the PI3K-AKT pathway. This promotes the progression and proliferation of HCC.

between the NAT10 and DDIAS mRNA was also verified. Furthermore, previous studies have shown that NAT10 is crucial for DNA damage repair mechanisms by facilitating the histone acetylation of P53²⁸ and CW-type zinc finger structural protein 2, which are both proteins involved in the DNA damage response²⁹. The novel stress-induced gene, DNA damage-induced inhibitor of apoptosis (DDIAS; hNoxin), is a critical component in human cells that plays a role in protecting against cell death and promoting DNA repair. This protein is a human counterpart to a similar protein found in mice, known as Noxin. Through its anti-apoptotic properties, DDIAS helps to ensure the survival of cells under stressful conditions such as DNA damage. In addition to its role in DNA repair, DDIAS is also involved in regulating the cell cycle and apoptosis. Overall, the discovery of DDIAS sheds light on the intricate mechanisms that human cells utilize to protect themselves from damage and maintain their integrity. By understanding the functions of this stress-induced gene, researchers can potentially develop new strategies for enhancing cellular defense systems and preventing cell death. This knowledge may also lead to insights into diseases and conditions that involve cell cycle dysregulation or defective DNA repair mechanisms.

Furthermore, it has been discovered that pancreatic and lung cancer cells express DDIAS^{30–32}. Studies have demonstrated that DDIAS plays a central role in cancers such as HCC³⁰. Nevertheless, the structural domains of post-translational modifications, including phosphorylation, methylation, and acetylation, have not been examined in the current functional investigation of DDIAS. In the present study, we discovered that NAT10 acetylated DDIAS mRNA enhanced DDIAS translation efficiency and thus promoted the malignant progression of HCC. Concomitantly, DDIAS levels in HCC were noticeably higher than in normal tissues.

In addition, According to our findings, patients with HCC who had higher DDIAS levels had a lower probability of overall survival as well as disease-free survival. Sk-Hep-1 and HCCLM3 cell migration, invasion, and proliferation were all markedly suppressed by DDIAS knockdown. These results indicated that DDIAS can effectively regulate HCC progression in an N4-acetylcytidine-dependent manner.

The PI3K-AKT pathway is a crucial intracellular signaling system that aids in numerous cellular functions such as growth, angiogenesis, metabolism, proliferation, and cell survival by responding to external stimuli³¹. The PI3K-AKT pathway is crucial in the regulation of HCC progression. Activation of this pathway can notably suppress apoptosis and effectively control the synthesis of translation-related proteins, along with cell cycle progression, in tumour cells^{32,33}. The AKT/mTOR signaling pathway has been reported to correlate with liver fibrosis, which plays a crucial role in regulating liver pathophysiology³⁴. Based on bioinformatics analysis and a review of related studies¹⁸, we hypothesized that NAT10 could potentially regulate the PI3K-AKT pathway in HCC. Results indicate that DDIAS affects the PI3K-AKT pathway, which in turn affects the progression of HCC. This can be demonstrated by the reduced activation of the PI3K-AKT pathway following the knockdown of DDIAS. In a similar manner, the knockdown of NAT10 also affected the activation of the PI3K-AKT pathway. In the end, our findings indicated that the overexpression of DDIAS successfully mitigated the effects of NAT10 depletion on cellular invasion, migration, and proliferation. We found that NAT10 knockdown-induced PI3K AKT pathway modulation was reversed by DDIAS overexpression. Our findings thus indicate that NAT10 encouraged the formation of HCC via modulating the ac4C-DDIAS-PI3K-Akt pathway, so providing a unique means of influencing the progression of HCC. More research is necessary even though this study showed how

NAT10 controls HCC. First, due to the prevailing circumstances, it was not possible to conduct any additional animal experiments in this study to verify the in vitro findings. However, to address this constraint, we collected human tissue samples of HCC from our hospital as an additional supplement. Moreover, past studies have shown that DDIAS can be pharmacologically or genetically suppressed to help in the development of anticancer drugs³⁵, however, the DDIAS inhibitor has not yet been discovered for the treatment of HCC.

In conclusion, we show that NAT10 expression is significantly upregulated in HCC based on our data. Patients diagnosed with HCC and elevated levels of NAT10 experienced reduced overall survival rates, indicating that NAT10 actively facilitated HCC development. NAT10 modulated the ac4C-DDIAS-PI3K-AKT pathway to govern the evolution of HCC mechanistically. These results offer fresh insights into targeted treatment for HCC.

Data availability

The datasets used and/or analysed during the current study are available from the corresponding author on reasonable request.

Received: 24 May 2024; Accepted: 30 April 2025

Published online: 19 May 2025

References

- Sung, H. et al. Global Cancer statistics 2020: GLOBOCAN estimates of incidence and mortality worldwide for 36 cancers in 185 countries. *CA Cancer J. Clin.* **71**, 209–249 (2021).
- Petrick, J. L. et al. International trends in hepatocellular carcinoma incidence, 1978–2012. *Int. J. Cancer.* **147**, 317–330 (2020).
- Llovet, J. M. et al. Hepatocellular carcinoma. *Nat. Rev. Dis. Primers.* **7**, 6 (2021).
- Roderburg, C., Özdirik, B., Wree, A., Demir, M. & Tacke, F. Systemic treatment of hepatocellular carcinoma: from Sorafenib to combination therapies. *Hepat. Oncol.* **7** (2), HEP20 (2020).
- Xie, D. Y., Ren, Z. G., Zhou, J., Fan, J. & Gao, Q. 2019 Chinese clinical guidelines for the management of hepatocellular carcinoma: updates and insights. *Hepatobiliary Surg Nutr.* **9**, 452–463 (2020).
- Chen, Z. et al. Recent progress in treatment of hepatocellular carcinoma. *Am. J. Cancer Res.* **10**, 2993–3036 (2020).
- Gunasekaran, G., Bekki, Y., Lourdusamy, V. & Schwartz, M. Surgical treatments of hepatobiliary cancers. *Hepatology* **73** (1), 128–136 (2021).
- Pogribny, I. P. & Rusyn, I. Role of epigenetic aberrations in the development and progression of human hepatocellular carcinoma. *Cancer Lett.* **342**, 223–230 (2014).
- Nishida, N. & Goel, A. Genetic and epigenetic signatures in human hepatocellular carcinoma: a systematic review. *Curr. Genomics.* **12**, 130–137 (2011).
- Wiener, D. & Schwartz, S. The epitranscriptome beyond m6A. *Nat. Rev. Genet.* **22**, 119–131 (2021).
- Arango, D. et al. Acetylation of cytidine in mRNA promotes translation efficiency. *Cell* **175**, 1872–1886e24 (2018).
- Jin, C. et al. Acetyltransferase NAT10 regulates the Wnt/ β -catenin signaling pathway to promote colorectal cancer progression via ac4C acetylation of KIF23 mRNA. *J. Exp. Clin. Cancer Res.* **41**, 345 (2022).
- Yang, Q. et al. N4-Acetylcytidine drives Glycolysis addiction in gastric Cancer via NAT10/SEPT9/HIF-1 α positive feedback loop. *Adv. Sci. (Weinh.)* **10**, e2300898 (2023).
- Zhang, Y. et al. NAT10 promotes gastric cancer metastasis via N4-acetylated COL5A1. *Signal. Transduct. Target. Ther.* **6**, 173 (2021).
- Liu, D., Yang, X. & Wang, X. Neutrophil extracellular traps promote gastric cancer cell metastasis via the NAT10-mediated N4-acetylcytidine modification of SMYD2. *Cell. Signal.* 111014 (2023).
- Feng, Z. H. et al. RIN1 promotes renal cell carcinoma malignancy by activating EGFR signaling through Rab25. *Cancer Sci.* **108**, 1620–1627 (2017).
- Zhang, S. et al. Linc00662 m6A promotes the progression and metastasis of pancreatic cancer by activating focal adhesion through the GTF2B-ITGA1-FAK pathway. *Am. J. Cancer Res.* **13**, 1718–1743 (2023).
- Zhang, Y. et al. NAT10 acetylates BCL-XL mRNA to promote the proliferation of multiple myeloma cells through PI3K-AKT pathway. *Front. Oncol.* **12**, 967811 (2022).
- Llovet, J. M. et al. Immunotherapies for hepatocellular carcinoma. *Nat. Rev. Clin. Oncol.* **19**, 151–172 (2022).
- Llovet, J. M. et al. Locoregional therapies in the era of molecular and immune treatments for hepatocellular carcinoma. *Nat. Rev. Gastroenterol. Hepatol.* **18**, 293–313 (2021).
- Llovet, J. M., Montal, R., Sia, D. & Finn, R. S. Molecular therapies and precision medicine for hepatocellular carcinoma. *Nat. Rev. Clin. Oncol.* **15**, 599–616 (2018).
- Larrieu, D. et al. Inhibition of the acetyltransferase NAT10 normalizes progeric and aging cells by rebalancing the Transportin-1 nuclear import pathway. *Sci. Signal.* **11**, eaar5401 (2018).
- Shrimp, J. H. et al. Remodelin is a cryptic assay interference chemotype that does not inhibit NAT10-Dependent cytidine acetylation. *ACS Med. Chem. Lett.* **12**, 887–892 (2021).
- Ma, R. et al. Up regulation of NAT10 promotes metastasis of hepatocellular carcinoma cells through epithelial-to-mesenchymal transition. *Am. J. Transl Res.* **8**, 4215–4223 (2016).
- Tan, Y. et al. Loss of nucleolar localization of NAT10 promotes cell migration and invasion in hepatocellular carcinoma. *Biochem. Biophys. Res. Commun.* **499**, 1032–1038 (2018).
- Wang, L. et al. The emerging roles of ac4C acetylation ‘writer’ NAT10 in tumorigenesis: A comprehensive review. *Int. J. Biol. Macromol.* **254**, 127789 (2024).
- Jin, G., Xu, M., Zou, M. & Duan, S. The processing, gene regulation, biological functions, and clinical relevance of N4-Acetylcytidine on RNA: A systematic review. *Mol. Ther. Nucleic Acids.* **20**, 13–24 (2020).
- Liu, X. et al. NAT10 regulates p53 activation through acetylating p53 at K120 and ubiquitinating Mdm2. *EMBO Rep.* **17**, 349–366 (2016).
- Liu, H. Y. et al. Acetylation of MORC2 by NAT10 regulates cell-cycle checkpoint control and resistance to DNA-damaging chemotherapy and radiotherapy in breast cancer. *Nucleic Acids Res.* **48**, 3638–3656 (2020).
- Zhang, Z. Z., Huang, J., Wang, Y. P., Cai, B. & Han Z.-G. NOXIN as a cofactor of DNA polymerase-primase complex could promote hepatocellular carcinoma. *Int. J. Cancer.* **137**, 765–775 (2015).
- Bilanges, B., Posor, Y. & Vanhaesebroeck, B. PI3K isoforms in cell signalling and vesicle trafficking. *Nat. Rev. Mol. Cell. Biol.* **20**, 515–534 (2019).
- Sun, E. J., Wankell, M., Palamuthusingam, P., McFarlane, C. & Hebbard, L. Targeting the PI3K/Akt/mTOR pathway in hepatocellular carcinoma. *Biomedicine* **9**, 1639 (2021).
- Tian, L. Y., Smit, D. J. & Jücker, M. The role of PI3K/AKT/mTOR signaling in hepatocellular carcinoma metabolism. *Int. J. Mol. Sci.* **24**, 2652 (2023).

34. Zhang, H. et al. KIF18A inactivates hepatic stellate cells and alleviates liver fibrosis through the TTC3/Akt/mTOR pathway. *Cell. Mol. Life Sci.* **81** (1), 96 (2024).
35. Im, J. Y., Kang, M. J., Kim, B. K., Won, M. & DDIA5 DNA damage-induced apoptosis suppressor, is a potential therapeutic target in cancer. *Exp. Mol. Med.* **55**, 879–885 (2023).

Author contributions

H.H., Y.M., Y.Y.G. conceived and designed the research study. Y.T., L.S.W. and E.-H.C. contributed to the writing of the manuscript and participated in the experiments. D.J.Y., S.Z. contributed to the sample collection and interpretation of the data. W.Q.C., Y.Z.H. performed the statistical analysis. HH reviewed and supervised this paper. All authors read and approved the final manuscript.

Funding

Supported by: (1) Natural Science Foundation of Jiangsu Province, BK20191142. (2) Jiangnan University Hospital Clinical Medical Research Project, LCYJ202321.

Declarations

Competing interests

The authors declare no competing interests.

Additional information

Supplementary Information The online version contains supplementary material available at <https://doi.org/10.1038/s41598-025-00707-x>.

Correspondence and requests for materials should be addressed to Y.G., Y.M. or H.H.

Reprints and permissions information is available at www.nature.com/reprints.

Publisher's note Springer Nature remains neutral with regard to jurisdictional claims in published maps and institutional affiliations.

Open Access This article is licensed under a Creative Commons Attribution-NonCommercial-NoDerivatives 4.0 International License, which permits any non-commercial use, sharing, distribution and reproduction in any medium or format, as long as you give appropriate credit to the original author(s) and the source, provide a link to the Creative Commons licence, and indicate if you modified the licensed material. You do not have permission under this licence to share adapted material derived from this article or parts of it. The images or other third party material in this article are included in the article's Creative Commons licence, unless indicated otherwise in a credit line to the material. If material is not included in the article's Creative Commons licence and your intended use is not permitted by statutory regulation or exceeds the permitted use, you will need to obtain permission directly from the copyright holder. To view a copy of this licence, visit <http://creativecommons.org/licenses/by-nc-nd/4.0/>.

© The Author(s) 2025